

Concentration efficiency of doping in phosphors: Investigation of the copper- and aluminum-doped zinc sulfide

Lai Qi and Burtrand I. Lee^{a)}

School of Materials Science and Engineering, Clemson University, Clemson, South Carolina 29634

Xuejun Gu

Department of Physics and Astronomy, Clemson University, Clemson, South Carolina 29634

Mica Grujicic

Department of Mechanical Engineering, Clemson University, Clemson, South Carolina 29634

William D. Samuels and Gregory J. Exarhos

Department of Materials Science, Pacific Northwest National Laboratory, Richland, Washington 99352

(Received 28 July 2003; accepted 20 October 2003)

We studied the effect of dopant concentration in ZnS:Cu, Al phosphor. Photoluminescent (PL) intensity of the chemically etched phosphor particles increased up to 140%, which proved the existence of a dopant concentration gradient. Calculation revealed the quantitative relationship between the dopant concentration and the luminescent intensity by relating the concentration gradient to the PL intensity. The result showed that the most efficient concentration is 100 ppm copper and the concentration quenching starts at 152 ppm. © 2003 American Institute of Physics. [DOI: 10.1063/1.1633335]

ZnS:Cu, Al has widely been used as a green phosphor since its first application in (CRT) mass production in 1973.¹ The copper concentration is one of the key factors that directly influence the luminescent emission intensity. The luminescent intensity normally increases with increasing copper concentration up to a certain value and then decreases with further doping. This is a common phenomenon for most doped phosphors,^{2,3} called concentration quenching, which relates to the nonemissive cross relaxation between dopants.⁴

In the literature, the reported optimum copper concentration varies from 50 to 200 ppm.⁵⁻⁷ This discrepancy is understandable, because it is difficult to separate the concentration effect from other influencing factors, i.e., purity, crystallinity, particle morphology, contamination, etc. So far, reports of focused investigation of the concentration effect on luminescent intensity are rare. And in most cases, the average doping concentration was used, assuming a homogeneous distribution of the dopant. However, we found it is not so in the ZnS:Cu, Al we studied.

Up to now, the most effective and industrially adopted synthesis route for ZnS:Cu, Al is called solid-state-reaction (SSR).⁸ In this process, ZnS particles are prepared first and then mixed with solution of the activator salts and flux. The activator cations deposited on the ZnS particle surface diffuse into the particle matrix during the subsequent annealing treatment. The dopants will actually form concentration gradients, rather than uniform distributions. Any variation of the annealing conditions, i.e., temperature or time, will change the gradient shape and thus change the luminescent intensity, while the average concentration may remain the same. Therefore, average concentration may not truly relate to the luminescent properties.

In this work, we calculated the copper concentration gra-

dient in a commercial SSR-ZnS:Cu, Al particles (P22-GN4, Kasei Optonix, Ltd. Japan). The phosphor particles were etched by hydrochloric acid. The diameter of the etched particles could be controlled from 7.2 μm to 100 nm, as shown in Fig. 1. Similar etching treatment has been reported by Ozawa.⁹ Considering the incomplete penetration of electrons in cathodoluminescence,¹⁰ photoluminescence (PL) measurement (excitation wavelength, 375 nm) was adopted to characterize those etched particles. The average copper concentration was measured by the inductively coupled plasma spectroscopy (ICP). The surface copper concentration was estimated by the x-ray photoelectron spectroscopy (XPS). The concentration effect of copper on the luminescent intensity was specified by a coefficient, defined as coefficient of concentration efficiency (CCE).

In the course of this work, four assumptions were made. First, phosphor particles are spherical in shape. Second, the etching happened mainly at the particle surface and affected only a few atomic layers below the etched surface. Thus, the etched particles keep the same characteristics as they had before etching, i.e., the same structure, chemical composition, and density, etc. X-ray diffraction (XRD), as shown in Fig. 2, confirmed no significant structure change after etching. The missing of the peak at 27.5°, which relates to the stacking fault of the (111) plane, indicated that etching hap-

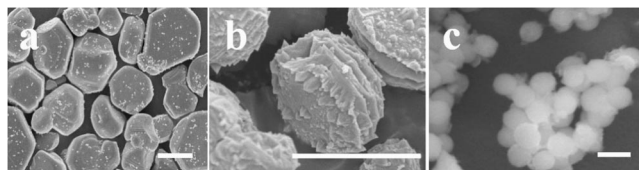


FIG. 1. Scanning electron micrographs of (a) the as-received; (b) 60 s etched, and (c) 14-min-etched particles. The scale bars represent 5 μm , 5 μm , and 100 nm, respectively.

^{a)}Electronic mail: burt.lee@ces.clemson.edu

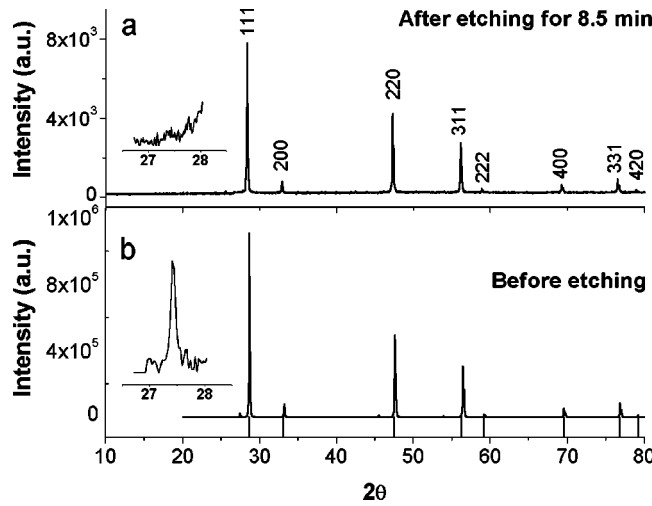


FIG. 2. X-ray diffraction patterns of (a) the 8.5 min etched, and (b) as-received particles. Insets: enlarged views of 27° – 28° . The vertical lines on the X axis are the standard cubic ZnS diffraction pattern (JCPDS 05-0566).

pened mainly at the grain boundary and particle surface. The third assumption is that the particles are basically free of surface defects due to the surface cleaning treatment in commercial production. The fourth assumption is that according to the XPS data and the experimental conditions, the influence of Cl^- on the PL emission of etched particles is not significant.

The diffusion of copper in a spherical particle is governed by the Fick's second law:^{11,12}

$$\frac{\partial C}{\partial t} = D \times \left(\frac{\partial^2 C}{\partial r^2} + \frac{2}{r} \times \frac{\partial C}{\partial r} \right),$$

where C and D are concentration and the diffusion coefficient, respectively. The diffusion coefficient could be treated as a constant for the low copper concentration (the average concentration is below 200 ppm by ICP). A general solution to the above equation is:

$$C_{r,t} = \frac{\alpha}{2\sqrt{\pi(Dt)^3}} \exp\left(-\frac{r^2}{4Dt}\right),$$

where α is the mass of copper deposited on the particle surface before annealing, and t is the annealing time. For the samples we studied, α and t have fixed values since they are already made. Thus, the solution equation can be simplified as:

$$C_r = A \exp[-(R-r)^2/B], \quad (1)$$

where R is the particle radius before etching; A and B are constants determined by the initial synthesis conditions.

To solve the constants A and B in Eq. (1), two boundary conditions are required. In this work, they are the surface concentration before etching (179 ppm), therefore $A = 179$ ppm, and the average concentration (140 ppm). The average concentration of copper, C_m , can be derived as $C_m = (3/R^3) \int_0^R C_r r^2 dr$. Replacing C_r with Eq. (1) gives

$$C_m = \frac{3AB}{2R^2} \left[\left(\frac{R\sqrt{\pi}}{\sqrt{B}} + \frac{\sqrt{B}\pi}{2R} \right) \operatorname{erf}\left(\frac{R}{\sqrt{B}}\right) + \exp\left(\frac{-R^2}{B}\right) - 1 \right] = 140 \text{ ppm}. \quad (2)$$

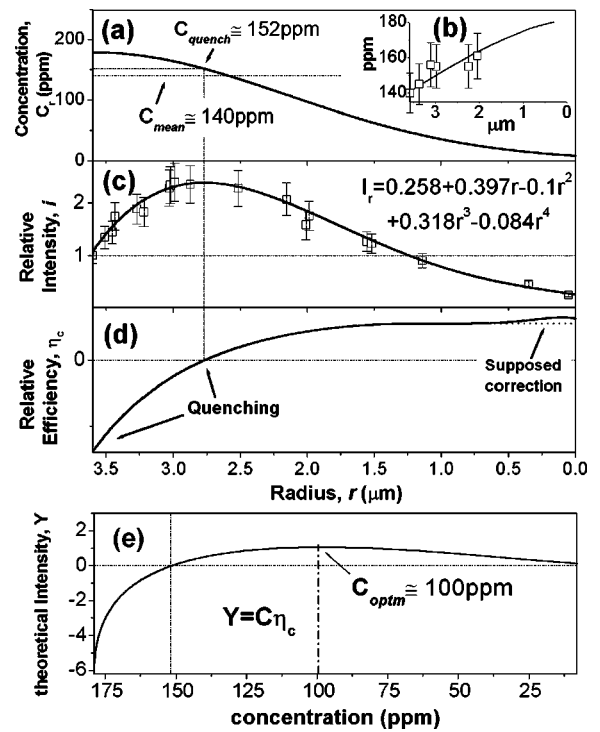


FIG. 3. Plot of functions (abscissa: particle radius, from particle surface to the center). (a) the calculated copper concentration gradient, C_{quench} is the quenching concentration, C_{mean} is the mean concentration; (b) the calculated mean concentration of etched particles based on the gradient in curve **a**; (c) the measured relative PL intensity and the polynomially fitted curve; (d) the calculated relative CCE curve; (e) the theoretical output intensity curve, C_{optm} is the optimized concentration.

Equation (2) was solved by iterative calculation, giving $B = 4.2 \mu\text{m}^2$. The calculated gradient curve $C_r = 179 \exp[-(3.6-r)^2/4.2]$ is shown as curve **a** in Fig. 3. Curve **b** is the calculated average concentration of etched particles, based on the gradient in curve **a**. The measured values agree with the calculation. Curve **c** is the polynomial simulation of the measured PL relative intensities. A 140% increase of the PL intensity was observed for the particles with $1 \mu\text{m}$ top surface etched away.

The observed luminescent intensity should be a function of a number of factors: $I_{em} = f(I_{ex}, M, X_{tal}, P, C_r, \dots)$, where $I_{em}, I_{ex}, M, X_{tal}, P, C_r$ are the emission intensity, excitation intensity, sample mass, crystallinity, purity, and doping concentration, respectively. For differently etched samples, all the variables, except C_r , were kept the same because I_{ex} and M were experimentally set to be constant. X_{tal} and P were supposed to have no change after etching. The only variation was the dopants distribution C_r . So, the last equation could be rewritten as: $I_{em} = H_c \times C_r$, where $H_c = f(I_{ex}, M, X_{tal}, P, C_r, \dots)/C_r$ is the CCE.

For a particle with radial concentration gradient C_r and radius of r' , the emission intensity $I_{r'}$ should be the sum of contribution from all the dopants within the particle: $I_{r'} = \int_0^{r'} H_c C_r 4\pi r^2 dr$. The observed PL intensity of a sample should be the sum of contribution from all the particles: $I_{r'} = n_{r'} \int_0^{r'} H_c C_r 4\pi r^2 dr$, where $n_{r'}$ is the number of particles with radius of r' . The product of particle number and single particle volume was constant because of the same sample weight loading for each PL measurement and the assumption of constant density. Therefore, $n_{r'} \times V_{r'} = \text{constant}$, where

$V_{r'}$ is the particle volume. The relative PL intensity $i_{r'}$ is defined as:

$$i_{r'} = I_{r'} / I_R, \quad (3)$$

where $I_{r'}$ is the measured PL intensity of an etched sample; I_R is the measured PL intensity of the nonetched sample. Therefore, Eq. (3) becomes

$$i_{r'} = \beta r'^{-3} \times \int_0^{r'} H_c C_r 4\pi r^2 dr, \quad (4)$$

where

$$\beta = R^3 \times \left(\int_0^R H_c C_r 4\pi r^2 dr \right)^{-1}$$

is a constant.

To separate H_c , Eq. (4) was differentiated by radius, giving

$$H_c = \frac{1}{\beta} \left(\frac{di_{r'}}{dr'} \times \frac{r'}{3C_{r'}} + \frac{i_{r'}}{C_{r'}} \right).$$

As defined, H_c should give absolute values. However, in practical cases, it is impossible to calculate the β . Thus, the relative CCE η_c is defined as: $\eta_c = H_c \times \beta$.

Therefore,

$$\eta_c = \frac{di_{r'}}{dr'} \times \frac{r'}{3C_{r'}} + \frac{i_{r'}}{C_{r'}}. \quad (5)$$

The derivative $di_{r'}/dr'$ could be derived from the fitting equation shown in curve *c* of Fig. 3. Thus, Eq. (5) could be calculated, which is shown as curve *d*.

In Fig. 3, the concentration, PL intensity, and the doping efficiency are related to each other through the abscissa of radius. The relative CCE becomes zero at the concentration that gives the highest PL intensity (152 ppm) because of the fact that any further doping beyond this point decreases the total intensity, which indicates a negative CCE. The concentration quenching starts from this point, because increased cross relaxation will cause more light to be absorbed than emitted in those overdoped portions. As the concentration decreases, the efficiency increases gradually to a limit. The

explanation is: as the doping concentration decreases, the distance between dopants increases. The chance of nonradiative relaxation between dopants decreases, so the CCE goes up. The highest efficiency should be at the zero concentration, where the cross relaxation is null. The instrumental errors became significant when radius approached zero. A correction of the CCE curve at radius of zero is suggested (dotted line).

Based on a homogeneous distribution model, another function, the theoretical output intensity Y is defined as: $Y = C \times \eta_c$, which is shown as curve *e* in Fig. 3, indicating that the optimum doping concentration is about 100 ppm.

It was found that although the comprehensive properties had been optimized, the commercial ZnS:Cu, Al particles still have a 1 μm overdoped surface layer. Luminescent intensity was significantly improved when this layer was etched away. This method and equations above could also be applied to studies of other similar materials.

The authors thank Dr. Sergey Bukesov for the helpful discussion and the Kasei Optonix, Ltd. (Japan) for providing the samples and permission of publishing the data.

- ¹S. Shionoya, and W. M. Yen, *Phosphor Handbook* (CRC, Boca Raton, FL, 2000), p. 841.
- ²E. Danielson, J. H. Golden, E. W. McFarland, C. M. Reaves, W. H. Weinberg, and X. D. Wu, *Nature* (London) **389**, 944 (1997).
- ³G. Blasse, and B. C. Grabmaier, *Luminescent Materials* (Springer, Berlin, 1994), p. 140.
- ⁴T. Maruyama, H. Yamada, T. Mochizuki, K. Akimoto, and E. Yagi, *J. Cryst. Growth* **214/215**, 954 (2000).
- ⁵C. Onose, S. Jinga, and C. Onose, *Proc. SPIE* **4068**, 72 (2000).
- ⁶E.-J. Popovici, F. Forgaciu, C. Ciocan, L. Pascu, D. Angelescu, and C. Postolache, *Proc. SPIE* **4068**, 130 (2000).
- ⁷Y. Y. Chen, J. G. Duh, B. S. Chiou, and C. G. Peng, *Thin Solid Films* **392**, 50 (2001).
- ⁸G. R. Fonda and F. Seitz, *Preparation and Characteristics of Solid Luminescent Materials* (Wiley, London, 1948), p. 208.
- ⁹L. Ozawa, *Cathodoluminescence, Theory and Applications* (VCH, Weinheim, Germany, 1990), p. 18.
- ¹⁰H. Bechtel, W. Czarnojan, M. Haase, W. Mayr, and H. Nikol, *Philips J. Res.* **50**, 433 (1996).
- ¹¹J. Crank, *The Mathematics of Diffusion* (Oxford University Press, Fair Lawn, NJ, 1975).
- ¹²H. S. Carslaw and J. C. Jaeger, *Conduction of Heat In Solids* (Oxford University Press, Fair Lawn, NJ, 1959), p. 230.